Approximation of resonance functions for real trajectories in the impact broadening theory. Part 1. Electrostatic interactions, real parts

N.N. Lavrent'eva[1] and V.I. Starikov[1,2]

[1] *Institute of Atmospheric Optics, Siberian Branch of the Russian Academy of Sciences, Tomsk*
[2] *Tomsk State University of Control Systems and Radioelectronics*

Received April 14, 2005

An analytical formula is proposed for approximation of resonance functions in the broadening theory and for shift of molecular spectral lines. This formula accounts for the trajectory curvatures of colliding particles. The equation obtained is a part of a power series in terms of hyperbolic tangents th(z). The coefficients of this series are determined for the case of trajectories defined by the Lennard–Jones (6–12) intermolecular interaction potential. This paper presents the coefficient values for the case of electrostatic interactions. Real parts of the resonance functions needed for calculation of broadening coefficients are considered.

Introduction

The knowledge of line profile parameters, such as coefficients of broadening (γ) and shift (δ) by pressure of different gases, is necessary in many applications, particularly, in reliable choice of frequency for sensing molecular impurities in the Earth atmosphere. They also contain information on the intermolecular interaction potential depending on the polarizability, as well as dipole, quadrupole, and other moments of colliding molecules.

To determine δ and γ numerically, it is necessary to know the truncation function $S(b)$, which is defined in terms of the time perturbation theory and depends on matrix elements of the intermolecular potential in the basis of vibration-rotation wave functions of colliding molecules.[1–3] The multiplier

$$F^{(n)}_{l_1 l_2 LM}(\omega) = \int_{-\infty}^{+\infty} \mathrm{d}t e^{i\omega t} C_{LM}[r(t)] B^{(n)}_{l_1 l_2}[r(t)], \qquad (1)$$

entering into the expression for the matrix elements, is the Fourier transform of the intermolecular potential coefficients. In Eq. (1), l_1 and l_2 determine the order of the tensor of physical quantities of colliding molecules 1 and 2, respectively (e.g. 2^l-pole moments); C_{LM} are spherical harmonics depending on the intermolecular distance $r(t)$; t is time; index n discriminates interactions of different types but of the same tensor nature; and, finally, $B[r(t)]$ determines the $r(t)$-dependence. Commonly, δ and γ are calculated in the straight-line trajectory approximation, in which, if molecules interact in the x–y-plane, where $x(t) = b$, $y(t) = vt$, and $z(t) = 0$, the $r(t)$-dependence is determined by the relation $r(t) = (b^2 + vt^2)^{1/2}$, where v is the relative velocity of molecules and b is the impact parameter. In this approximation, resonance functions have been obtained in a series of works,[1–7] for example, functions $f_1(k)$, $f_2(k)$, and $f_3(k)$ [real parts $f_{l_1 l_2}(k)$ of resonance functions $F(k)$] for dipole-dipole ($l_1 = l_2 = 1$), dipole-quadrupole ($l_1 = 1$, $l_2 = 2$), and quadrupole-quadrupole ($l_1 = l_2 = 2$) interactions have the following forms:

$$f_1(k) = (k^4/4)[K_2(k)^2 + 4K_1(k)^2 + 3K_0(k)^2],$$

$$f_2(k) = (k^6/64)[K_3(k)^2 + 6K_2(k)^2 + 15K_1(k)^2 + 10K_0(k)^2],$$

$$f_3(k) = (k^8/2304)[K_4(k)^2 + 8K_3(k)^2 + 28K_2(k)^2 + 56K_1(k)^2 + 35K_0(k)^2]. \qquad (2)$$

Here the adiabaticity parameter $k = 2\pi cb(\omega_{ii'} + \omega_{22'})/v$ depends on rovibrational (RV) frequencies of transitions $\omega_{ii'} = E_i - E_{i'}$ and $\omega_{22'} = E_2 - E_{2'}$ (E_i and E_2 are the RV-levels of molecules 1 and 2); $K_n(k)$ are Bessel functions.

In a number of cases, the straight-line trajectory approximation is not correct. For example, in Refs. 8 and 10, the effect of trajectory bending from a straight-line on H_2O-level shifts caused by a pressure of different buffer gases was estimated. As was shown, accounting for trajectory curvatures of colliding particles can introduce up to 40% corrections into shifts of water vapor absorption levels providing the shifts are caused by pressure of rare gases.

In Ref. 9, a parabolic trajectory model was suggested, in which the $r(t)$-dependence was determined as $r(t) = (r_c^2 + v_c'^2 t^2)^{1/2}$. Here r_c is the distance of the closest approach between molecules; v_c' is the apparent relative velocity, determined for the Lennard–Jones (6–12) potential. The trajectory of colliding particles looks like a parabola. Resonance

0235-6880/05/09 729-06 $02.00

functions, obtained in this approximation, depend on r_c and v_c'; some of them are presented in Ref. 9.

The most consistent technique for calculation of resonance functions $f(k)$, which accounts for trajectory curvature of colliding particles determined by arbitrary intermolecular interaction potential, was reported in Refs. 10 and 11 (see also Ref. 8). In these works, a common expression for the real part of $f_{l_1 l_2}(k)$ was obtained. For particular values of k, these functions can be calculated only numerically.

The goal of our work was to obtain analytical formulas of resonance functions for different values of parameters of the isotropic part of intermolecular interaction Lennard–Jones 6–12 potential on the base of common expression for resonance functions (Refs. 8, 10, 11). Numerous data on the potential parameters were obtained for different pairs of interacting particles.

Expansion into series in terms of hyperbolic tangents th(z)

In Refs. 10 and 11, definition of resonance functions bases on dynamic equations, which are well known from classical mechanics.[14] As follows from the equations, the time dependence of the distance $r(t)$ is determined by the equation

$$\frac{dr(t)}{dt} = \{2[E - U(r)]/\mu - M^2/\mu^2 r^2\}^{1/2}, \qquad (3)$$

where $E = mv^2/2$ is energy; $M = mbvm^{-1} = m_1^{-1} + m_2^{-1}$ is the reduced mass of particles; $U(r)$ is the interaction potential. A direct calculation of the Fourier transform (1) results in the following equation for resonant functions:

$$f_{l_1 l_2}(k) = \frac{2(2L)!B}{(2l_1+1)!(2l_2+1)!} \times$$

$$\times \sum_{\substack{m \\ L+m=2p}} \frac{(L+m-1)!!(L-m-1)!!}{(L+m)!!(L-m)!!} \times$$

$$\times \left\{ \int_1^\infty dy \frac{\cos[A_0(y)k_c + m\sqrt{1-V(r_c)}A_2(y)]}{y^L \sqrt{y^2 - 1 - V(r_c) - y^2 V(yr_c)}} \right\}^2, \qquad (4)$$

where

$$A_n(y) = \int_1^y \left\{ \frac{dz}{z^{n-1}\sqrt{z^2 - 1 - V(r_c) - z^2 V(zr_c)}} \right\}^2; \qquad (5)$$

B is the normalization factor chosen so that

$$f_{l_1 l_2}(k) = 1;\ k_c = 2\pi c r_c(\omega_{ii'} + \omega_{22'})/v;$$

parameter r_c is determined from solution of equation

$$(b/r_c)^2 = 1 - V(r_c), \qquad (6)$$

and

$$V(r) = 2U(r)/mv^2.$$

For the Lennard–Jones 6–12 potential

$$U(r) = 4\varepsilon\left\{-\left(\frac{\sigma}{r}\right)^6 + \left(\frac{\sigma}{r}\right)^{12}\right\}, \qquad (7)$$

Eq. (6) takes the form

$$\lambda\{\beta^{12} - \beta^6\} + (b^*)^2\beta^2 - 1 = 0, \qquad (8)$$

where

$$\lambda = 8\varepsilon/mv^2;\ \beta = (\sigma/r_c);\ b^* = b/\sigma. \qquad (9)$$

For potential $U(r)$ of an arbitrary type, $f_{l_1 l_2}(k)$ can be calculated only numerically. In special case, for $U(r) = 0$, resonance functions $f_{l_1 l_2}(k)$ in the form (4) turn to well known Eqs. (2) in the straight-line trajectory approximation. The shapes of $f_1(x)$, $f_2(x)$, and $f_3(x)$ ($x \equiv k$) are shown in Figs. 1–3, respectively.

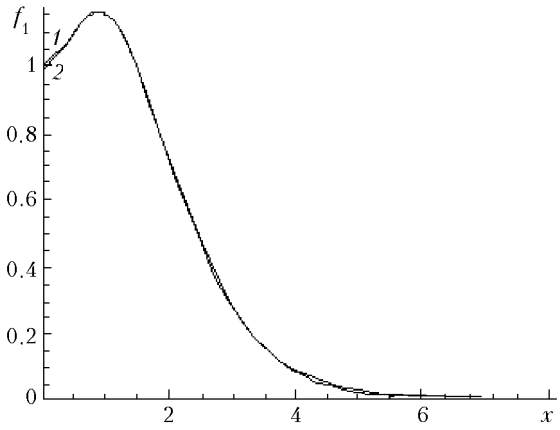

Fig. 1. True (Eq. (2)) (curve *1*) ($f_1(x = 0) = 1$) and model (Eq. (12)) (curve *2*) resonance functions $f_1(x)$.

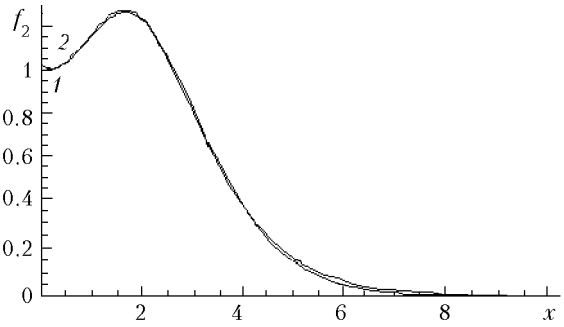

Fig. 2. True (Eq. (2)) (curve *1*) ($f_2(x = 0) = 1$) and model (Eq. (12)) (curve *2*) resonance function $f_2(x)$.

The curves are modeled well by the truncated series

$$f^{(m)}(x) = a_0 + a_1\text{th}(z) + a_2\text{th}^2(z) + a_3\text{th}^3(z),$$
$$z = \alpha(x - x_e), \qquad (10)$$

where a_0, a_1, a_2, a_3, α, and x_e are defined from the condition of the best agreement (in terms of least-squares method) between the model curve $f^{(m)}(x)$ and the exact one $f(x)$ specified by Eqs. (2). As it follows from the analysis, a_2 and a_3 can be correlated and

one of them must be fixed, e.g., at zero. This results in two equivalent representations of resonant functions:

$$f^{(m)}(x) = a_0 + a_1\mathrm{th}(z) + a_2\mathrm{th}^2(z), \quad (11)$$

$$f^{(m)}(x) = a_0 + a_1\mathrm{th}(z) + a_3\mathrm{th}^3(z). \quad (12)$$

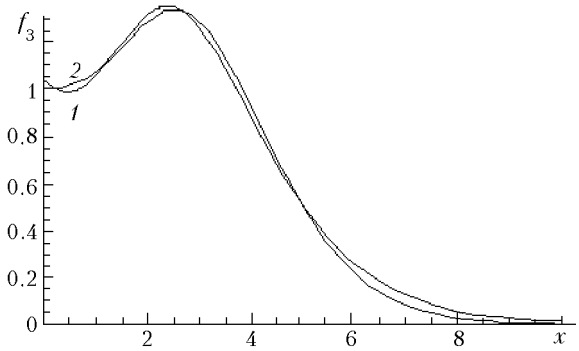

Fig. 3. True (Eq. (2)) (curve *1*) ($f_3(x = 0) = 1$) and model (Eq. (12)) (curve *2*) resonance function $f_3(x)$.

In Eq. (11), $a_0 = -a_1 - a_2$ for $f^{(m)}(x)$ and in Eq. (12) $a_0 = -a_1 - a_3$ for $f^{(m)}(x)$. Such selection of a_0 provides for correct asymptotics of resonance functions at large x. Model curves $f^{(m)}(x)$ (12) for cases of straight-line trajectories are also presented in Figs. 1–3. A close agreement between curves, specified by the model and exact resonance functions, is evident.

Application of Eqs. (11) and (12) is meaningless in cases of straight-line trajectories; however, model curves (11) and (12) are turned to be applicable for approximation of exact functions of type (4) as well.

Calculation of model function parameters

As is mentioned above, the values of $f_{l_1l_2}(x)$ for potential $U(r)$ of an arbitrary type can be found only numerically. We calculated the values of resonance functions $f_{l_1l_2}(x)$ (l_1, l_2 = 1, 2, and 3) for x between 0 and 7.9 with a step of 0.1 for $0 \le x \le 1.4$ and 0.5 for $1.4 \le x \le 7.9$. The isotropic interaction potential in form (7) was used; $\lambda = 0.3$, 0.7, 1.2, 1.7 and $\beta = 0$, 0.3, 0.5, 0.7, 0.75, 0.8, 0.85, 0.9, 0.95, 0.98, and 1 were taken for calculations. To simulate exact functions, the function $f^{(m)}(x)$ from Eq. (12) was chosen. Its coefficients depend on λ and β of the potential (7), hence

$$f^{(m)}_{l_1l_2}(x, \lambda, \beta) = a_1(\lambda, \beta)(\mathrm{th}[z(\lambda, \beta)] - 1) + a_3(\lambda, \beta)(\mathrm{th}^3[z(\lambda, \beta)] - 1), \quad (13)$$

$$z(\lambda, \beta) = \alpha(\lambda, \beta)[x - x_e(\lambda, \beta)].$$

For every fixed pair of λ and β, the coefficients in Eq. (13) were defined by the least-squares method from the fitting $f^{(m)}_{l_1,l_2}(x,\lambda,\beta)$ (13) to $f_{l_1,l_2}(x,\lambda,\beta)$ (4). Tables 1–3 present the coefficients of $f_1^{(m)}$, $f_2^{(m)}$, and $f_3^{(m)}$, respectively.

Table 1. Values of the $f_1^{(m)}(x, \lambda, \beta)$ resonance function parameters for the Lennard–Jones 6–12 potential

λ	β	a_1	$-a_3$	α	x_e
0	0	0.4228	1.4975	0.6138	0.3682
0.2	0.3	0.4329	1.5031	0.6310	0.4107
0.7	0.3	0.4333	1.5035	0.6311	0.4114
1.2	0.3	0.4336	1.5040	0.6312	0.4121
1.7	0.3	0.4340	1.5044	0.6313	0.4128
0.2	0.5	0.4358	1.5067	0.6317	0.4162
0.7	0.5	0.4435	1.5165	0.6337	0.4303
1.2	0.5	0.4514	1.5265	0.6357	0.4445
1.7	0.5	0.4595	1.5370	0.6377	0.4587
0.2	0.7	0.4518	1.5255	0.6356	0.4459
0.7	0.7	0.5032	1.5899	0.6482	0.5357
1.2	0.7	0.5618	1.6678	0.6626	0.6277
1.7	0.7	0.6317	1.7636	0.6796	0.7231
0.2	0.75	0.4578	1.5310	0.6368	0.4578
0.7	0.75	0.5259	1.6140	0.6535	0.5780
1.2	0.75	0.6075	1.7207	0.6737	0.7022
1.7	0.75	0.7148	1.8643	0.6996	0.8325
0.2	0.8	0.4613	1.5311	0.6374	0.4674
0.7	0.8	0.5378	1.6161	0.6562	0.6113
1.2	0.8	0.6310	1.7302	0.6802	0.7596
1.7	0.8	0.7621	1.8943	0.7124	0.9125
0.2	0.85	0.4577	1.5173	0.6356	0.4665
0.7	0.85	0.5180	1.5608	0.6500	0.6078
1.2	0.85	0.5847	1.6213	0.6693	0.7509
1.7	0.85	0.6727	1.7112	0.6952	0.8938
0.2	0.9	0.4392	1.4764	0.6291	0.4418
0.7	0.9	0.4496	1.4192	0.6279	0.5257
1.2	0.9	0.4574	1.3749	0.6312	0.6155
1.7	0.9	0.4676	1.3444	0.6388	0.7091
0.2	0.95	0.3996	1.3969	0.6144	0.3695
0.7	0.95	0.3613	1.2265	0.5851	0.2989
1.2	0.95	0.3464	1.1194	0.5659	0.2591
1.7	0.95	0.3370	1.0411	0.5528	0.2409
0.2	1.0	0.3492	1.2886	0.5877	0.2092
0.7	1.0	0.4632	1.1875	0.5192	−0.2645
1.2	1.0	1.0471	1.4514	0.4739	−0.8032
1.7	1.0	3.0252	2.4069	0.4402	−1.4944

Figures 4 and 5 show β-dependences of $a_1(\lambda, \beta)$ and $a_3(\lambda, \beta)$ at different λ for $f_2^{(m)}$ responsible for the dipole-quadrupole interaction.

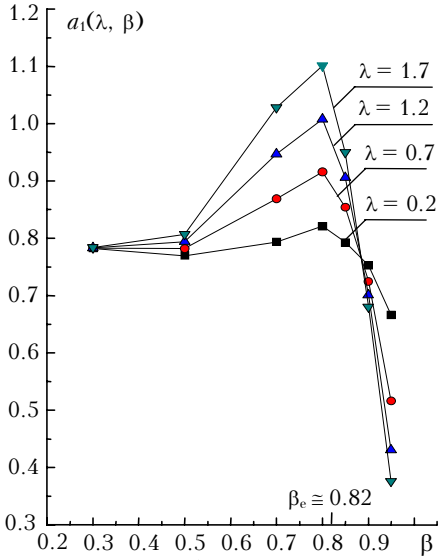

Fig. 4. Dependence of $a_1(\lambda, \beta)$ of the model resonance function $f_2^{(m)}$ on λ and β (Eq. (9)).

Table 2. Values of the $f_2^{(m)}(x, \lambda, \beta)$ resonance function parameters for the Lennard–Jones 6–12 potential

λ	β	a_1	$-a_3$	α	x_e
0	0	0.5883	1.7237	0.4858	0.9507
0.2	0.3	0.6092	1.7417	0.4912	0.9772
0.7	0.3	0.6098	1.7424	0.4912	0.9779
1.2	0.3	0.6104	1.7431	0.4913	0.9785
1.7	0.3	0.6109	1.7438	0.4913	0.9792
0.2	0.5	0.6135	1.7472	0.4914	0.9824
0.7	0.5	0.6249	1.7617	0.4921	0.9959
1.2	0.5	0.6364	1.7765	0.4928	1.0095
1.7	0.5	0.6480	1.7916	0.4934	1.0231
0.2	0.7	0.6364	1.7747	0.4925	1.0113
0.7	0.7	0.7074	1.8645	0.4959	1.0974
1.2	0.7	0.7836	1.9652	0.4989	1.1840
1.7	0.7	0.8662	2.0788	0.5013	1.2705
0.2	0.75	0.6442	1.7825	0.4927	1.0230
0.7	0.75	0.7357	1.8948	0.4963	1.1383
1.2	0.75	0.8344	2.0238	0.4990	1.2530
1.7	0.75	0.9418	2.1726	0.4997	1.3642
0.2	0.8	0.6479	1.7822	0.4923	1.0327
0.7	0.8	0.7463	1.8929	0.4946	1.1709
1.2	0.8	0.8488	2.0180	0.4954	1.3050
1.7	0.8	0.9543	2.1588	0.4924	1.4281
0.2	0.85	0.6396	1.7614	0.4906	1.0335
0.7	0.85	0.7106	1.8126	0.4889	1.1716
1.2	0.85	0.7762	1.8666	0.4862	1.3019
1.7	0.85	0.8361	1.9222	0.4808	1.4188
0.2	0.9	0.6069	1.7005	0.4863	1.0128
0.7	0.9	0.6016	1.6131	0.4761	1.1023
1.2	0.9	0.5970	1.5427	0.4677	1.1904
1.7	0.9	0.5936	1.4856	0.4605	1.2751
0.2	0.95	0.5358	1.5787	0.4778	0.9499
0.7	0.95	0.4274	1.3135	0.4521	0.9074
1.2	0.95	0.3685	1.1485	0.4333	0.8862
1.7	0.95	0.3315	1.0331	0.4187	0.8788
0.2	1.0	0.4202	1.3903	0.4624	0.8128
0.7	1.0	0.2490	1.0154	0.4120	0.4653
1.2	1.0	0.2316	0.8820	0.3759	0.1131
1.7	1.0	0.2996	0.8538	0.3478	−0.2763

Table 3. Values of the $f_3^{(m)}(x, \lambda, \beta)$ resonance function parameters for the Lennard–Jones 6–12 potential

λ	β	a_1	$-a_3$	α	x_e
0	0	0.7540	1.9291	0.3923	1.4380
0.2	0.3	0.7823	1.9613	0.3960	1.4642
0.7	0.3	0.7829	1.9620	0.3960	1.4649
1.2	0.3	0.7835	1.9628	0.3959	1.4655
1.7	0.3	0.7841	1.9636	0.3960	1.4662
0.2	0.5	0.7696	1.9482	0.3938	1.4534
0.7	0.5	0.7820	1.9645	0.3939	1.4673
1.2	0.5	0.7944	1.9810	0.3939	1.4812
1.7	0.5	0.8070	1.9979	0.3939	1.4951
0.2	0.7	0.7939	1.9786	0.3936	1.4832
0.7	0.7	0.8687	2.0766	0.3929	1.5709
1.2	0.7	0.9466	2.1841	0.3915	1.6572
1.7	0.7	1.0280	2.3029	0.3893	1.7416
0.2	0.8	0.8210	2.0033	0.3945	1.5222
0.7	0.8	0.9157	2.1144	0.3900	1.6628
1.2	0.8	1.0080	2.2342	0.3837	1.7954
1.7	0.8	1.1010	2.3669	0.3758	1.9212
0.2	0.85	0.7927	1.9587	0.3910	1.5085
0.7	0.85	0.8541	1.9994	0.3835	1.6527
1.2	0.85	0.9055	2.0378	0.3751	1.7857
1.7	0.85	0.9495	2.0757	0.3659	1.9094
0.2	0.9	0.7523	1.8856	0.3882	1.4902
0.7	0.9	0.7249	1.7655	0.3755	1.5925
1.2	0.9	0.7011	1.6673	0.3643	1.6893
1.7	0.9	0.6803	1.5853	0.3544	1.7809
0.2	0.95	0.6666	1.7407	0.3829	1.4308
0.7	0.95	0.5160	1.4126	0.3614	1.4113
1.2	0.95	0.4308	1.2099	0.3452	1.4106
1.7	0.95	0.3760	1.0696	0.3323	1.4211
0.2	1.0	0.5253	1.5138	0.3736	1.2983
0.7	1.0	0.2726	1.0323	0.3359	0.9956
1.2	1.0	0.1811	0.8232	0.3080	0.7081
1.7	1.0	0.1503	0.7145	0.2860	0.4074

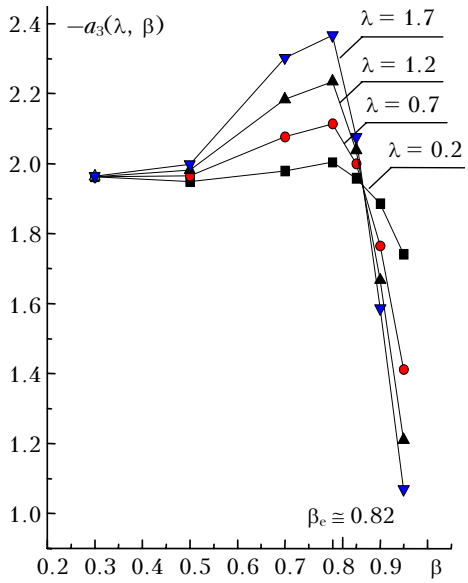

Fig. 5. Dependence of $-a_3(\lambda, \beta)$ of the model resonance function $f_2^{(m)}$ on λ and β (Eq. (9)).

Such a dependence is typical for all a_1, a_3, α, and x_e of all resonance functions. The correspondence of curve shapes (Figs. 4 and 5) to the potential shape in use is evident. At that, $\beta = 0$ corresponds to the straight-line trajectory approximation and β_e corresponds to the minimum point in the interaction potential.

Average thermal velocity approximation

Note, that λ and β in resonance functions (10)–(13) are not constants, they depend on the relative velocity v and the impact parameter b through Eqs. (9), i.e. $\lambda = \lambda(v, b)$ and $\beta = \beta(v, b)$. Average values of λ_{av} and β_{av} can be estimated, when using the average thermal velocity of molecules as v. In this approximation

$$\lambda_{av} = 8\varepsilon/(3k_B T),$$

where k_B is the Boltzmann constant and T is temperature. It is possible to estimate β_{av},

substituting b in Eq. (8) for b_0, obtained as a solution of the equation

$$S(b_0) = 1. \qquad (14)$$

The equation is used in the Anderson–Tsao–Curnutte theory (ATC)[1,2]; where the adiabaticity parameter k is zero for all virtual transitions. Table 4 presents λ_{av} and β_{av} for a number of water vapor mixtures important for practical use (see also Ref. 8).

Table 4. Parameters λ_{av} and β_{av} for H_2O collisions with different buffer gases (T = 273 K) for the Lennard–Jones 6–12 potential

System	ε/k_B, K	σ, Å	b_0, Å	λ_{av}	β_{av}
H_2O–H_2O	92.0[a]	3.23[a]	11.38	0.90	0.28
H_2O–H_2S	356.0[b]	2.72[b]	11.38	3.48	0.24
H_2O–SO_2	152.4	3.76	11.79	1.49	0.32
H_2O–N_2	109.4	3.51	4.70	1.07	0.83
H_2O–CO_2	132.0	3.86	6.40	1.29	0.62
H_2O–O_2	104.3	3.35	3.05	1.02	1.02
H_2O–He	31.54	3.0715	2.05	0.31	1.02
H_2O–Ne	58.86	3.17	2.59	0.58	1.05
H_2O–Ar	107.98	3.496	3.44	1.05	1.00
H_2O–Kr	129.01	3.59	3.78	1.26	0.99
H_2O–Xe	146.65	3.84	4.16	1.43	0.98

N o t e . Values of b_0 are taken from Ref. 8, where they are obtained as a solution of Eq. (14) with the adiabaticity parameter $k = 0$ for all virtual transitions. The Lennard–Jones potential parameters, marked by *a* and *b*, are taken from Ref. 12; the *b*-case corresponds to the definition of parameters from the second virial coefficient. Other potential parameters are taken from Ref. 13.

A closeness of β and β_e, which characterizes the maximal deviation from the straight-line trajectory approximation, is seen from Table 4 for all cases except for H_2O–H_2O, H_2O–SO_2, and, perhaps, H_2O–CO_2 mixtures. Resonance functions $f_2^{(m)}$ and $f_3^{(m)}$ were obtained for λ_{av} and β_{av}, indicated in Table 4 for H_2O–N_2 and H_2O–O_2. Figure 6 presents $f_2^{(m)}$ responsible for the dipole-quadrupole interaction.

The resonance function $f_2^{(m)}(\lambda = 0, \beta = 0)$, corresponding to the straight-line trajectory approximation, is shown here for comparison. A significant difference between the resonance functions is evident.

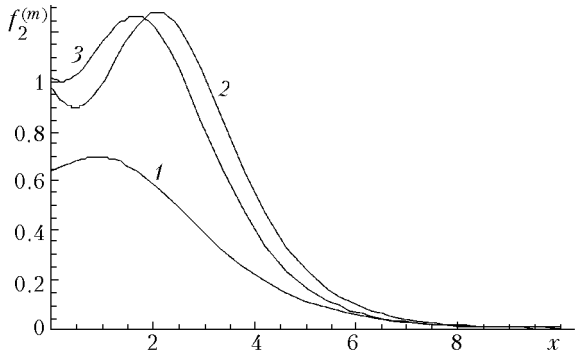

Fig. 6. Resonance functions $f_2^{(m)}(x, \lambda_{av}, \beta_{av})$ for H_2O–N_2 (*2*), H_2O–O_2 (*1*), and in the straight-line trajectory approximation (*3*). The approximation of the average thermal molecule velocity and Eq. (14) were used in calculations.

Extrapolation relationships for parameters of resonance functions

In the ATC technique, β values are defined through solution of Eq. (14) separately for each line. Therefore, the next step was a development of extrapolation relationships for $a_i(\lambda, \beta)$ (i = 1, 3), $\alpha(\lambda, \beta)$, and $x_e(\lambda, \beta)$. As is seen from Figs. 4 and 5, these relationships can differ for different intervals of β. In our work, we have treated the interval $0 \le \beta \le 0.9$ containing $\beta \approx \beta_e$, which corresponds to the minimum of molecule interaction potential; this minimum determines maximal deviation of resonance functions $f^{(m)}(\lambda, \beta)$ from $f_2^{(m)}(\lambda = 0, \beta = 0)$ in the straight-line trajectory model. Based on Figs. 4 and 5, we have chosen the following extrapolation formulas:

$$a_1(\lambda, \beta) = a_{10} + a_{1\lambda}\lambda/\mathrm{ch}[a_{1\beta}(\beta - \beta_{1e})],$$
$$a_3(\lambda, \beta) = a_{30} + a_{3\lambda}\lambda/\mathrm{ch}[a_{3\beta}(\beta - \beta_{3e})],$$
$$\alpha(\lambda, \beta) = \alpha_0 + \alpha_{\lambda\beta}\lambda\beta^2,$$
$$x_e(\lambda, \beta) = x_{e0} + x_{\lambda\beta}\lambda\beta^2. \qquad (15)$$

In Eqs. (15), a_{10}, a_{30}, α_0, and x_{e0} determine the resonance functions in the straight-line trajectory approximation; $a_{1\lambda}$, ..., $x_{\lambda\beta}$ have been obtained through $f_{l_1,l_2}^{(m)}(x,\lambda,\beta)$ fitting to the values of exact functions $f_{l_1,l_2}(x,\lambda,\beta)$ (Eq. (4)) at different x, λ, and β. The obtained parameters are presented in Table 5.

Table 5. Parameters of extrapolation formulas (15) for resonance functions

Function	a_{10}	$a_{1\lambda}$	$a_{1\beta}$	β_{1e}	α_0	$\alpha_{\lambda\beta}$
$f_1(x)$	0.4228±0.0180	0.1745±0.0286	6.08±0.74	0.994±0.061	0.6138±0.0105	0.0*
$f_2(x)$	0.5883±0.0500	0.1852±0.0075	7.18±0.63	0.898±0.061	0.4858±0.0530	0.0*
$f_3(x)$	0.754±0.014	0.2231±0.0132	8.96±0.55	0.8*	0.3923±0.0204	0.0*
	a_{30}	$a_{3\lambda}$	$a_{3\beta}$	β_{3e}	x_{e0}	$x_{\lambda\beta}$
$f_1(x)$	−1.4975±0.246	−0.112±0.007	13.26±0.86	0.773±0.004	0.368±0.006	0.315±0.007
$f_2(x)$	−1.724±0.047	−0.174±0.025	12.27±0.71	0.784±0.004	0.951±0.013	0.369±0.007
$f_3(x)$	−1.929±0.125	−0.342±0.026	16.92±0.26	0.763±0.002	1.438±0.032	0.382±0.014

*Fixed fitting parameter.

The root-mean-square deviation

$$\mathrm{RMS} = \left\{ \sum_{i}^{I} \frac{(f_i^{(m)} - f_i)^2}{(I - L)} \right\}^{1/2}$$

was chosen as the fitting quality factor. Here $f_i^{(m)}$ and f_i are the values of model and exact resonance functions; $I = 588$ is the total number of values; $L = 13$ is the number of fitted parameters in use. RMS is equal to $1.65 \cdot 10^{-3}$ for $f_1^{(m)}(x)$, $2.3 \cdot 10^{-3}$ for $f_2^{(m)}(x)$, and $2.6 \cdot 10^{-3}$ for $f_3^{(m)}(x)$.

Conclusion

The main results of this work are presented in Tables 1–3 and 5. The obtained parameters allow us to find the values of $f_1^{(m)}(x)$, $f_2^{(m)}(x)$, and $f_3^{(m)}(x)$ for some arbitrary x. As can be seen from Fig. 6, these values can differ essentially from those, obtained in the straight-line trajectory approximation.

Application of the developed technique to calculations of half-widths and line shifts of molecules will be described in the following works.

Acknowledgments

This work was supported by the Russian Foundation for Basic Research (Grant No. NSh 373.2003.5) and INTAS (Grant No. 03–51–3394).

References

1. P.W. Anderson, Phys. Rev. **76**, 647–661 (1949).
2. C.J. Tsao and B. Curnutte, J. Quant. Spectrosc. Radiat. Transfer **2**, 41–91 (1961).
3. R.P. Leavitt, J. Chem. Phys. **73**, 5432–5450 (1980).
4. C. Boulet, D. Robert, and L. Galatry, J. Chem. Phys. **65**, 5302–5314 (1976).
5. B.S. Frost, J. Phys. B.: Atom. Mol. Phys. **9**, 1001–1020 (1970).
6. R. Lynch, R. Gamache, and S.P. Neshyba, J. Chem. Phys. **105**, 5711–5721 (1996).
7. A.D. Bykov and N.N. Lavrent'eva, Atm. Opt. **4**, No. 7, 518–523 (1991).
8. A.D. Bykov, L.N. Sinitsa, and V.I. Starikov, *Experimental and Theoretical Methods in* H_2O *Molecule Spectroscopy* (Publishing House of Siberian Branch of the Russian Academy of Sciences, Novosibirsk, 1999), 376 pp.
9. D. Robert and J. Bonamy, J. de Phys. **40**, 923–943 (1979).
10. A.D. Bykov, N.N. Lavrent'eva, and L.N. Sinitsa, Atmos. Oceanic Opt. **5**, No. 9, 587–594 (1992).
11. A.D. Bykov, N.N. Lavrent'eva, and L.N. Sinitsa, Atmos. Oceanic Opt. **5**, No. 11, 728–730 (1992).
12. J. Girshfelder, Ch. Kertiss, and R. Bard, *Molecular Theory of Gases and Liquids* (Foreign Literature Press, Moscow, 1961).
13. B. Labani, J. Bonamy, D. Robert, J.-M. Hartman, and J. Taine, J. Chem. Phys. **84**, 4256–4267 (1986).
14. L.D. Landau and E.M. Lifshits, *Course of Theoretical Physics.* Vol. 1. *Mechanics* (Fizmatlit, Moscow, 1965), 203 pp.